Bat wing sensors support flight control

Susanne Sterbing-D'Angelo[a,1], Mohit Chadha[b,c], Chen Chiu[c], Ben Falk[c], Wei Xian[c], Janna Barcelo[c], John M. Zook[d], and Cynthia F. Moss[a,b,c]

[b]Program in Neuroscience and Cognitive Science, [c]Department of Psychology, and [a]Institute for Systems Research, University of Maryland, College Park, MD 20742; and [d]Department of Biological Sciences, Ohio University, Athens, OH 45701

Edited* by Jon H. Kaas, Vanderbilt University, Nashville, TN, and approved May 25, 2011 (received for review January 3, 2011)

Bats are the only mammals capable of powered flight, and they perform impressive aerial maneuvers like tight turns, hovering, and perching upside down. The bat wing contains five digits, and its specialized membrane is covered with stiff, microscopically small, domed hairs. We provide here unique empirical evidence that the tactile receptors associated with these hairs are involved in sensorimotor flight control by providing aerodynamic feedback. We found that neurons in bat primary somatosensory cortex respond with directional sensitivity to stimulation of the wing hairs with low-speed airflow. Wing hairs mostly preferred reversed airflow, which occurs under flight conditions when the airflow separates and vortices form. This finding suggests that the hairs act as an array of sensors to monitor flight speed and/or airflow conditions that indicate stall. Depilation of different functional regions of the bats' wing membrane altered the flight behavior in obstacle avoidance tasks by reducing aerial maneuverability, as indicated by decreased turning angles and increased flight speed.

Both the dorsal and ventral surfaces of the bat's wing membrane are covered with fine hairs protruding from dome-like structures. Whereas the existence of these hairs has been known for almost 100 y (1), their function has remained obscure and subject to speculation. One early hypothesis was that these hairs are the sensory receptors allowing bats to fly in complete darkness, which was refuted when Griffin and Galambos (2) showed in the early 1940s that bats have a sophisticated biological sonar system for spatial orientation. Subsequently, the domed wing hairs were a forgotten subject and have received little research attention (but see refs. 3 and 4).

The bat wing is a highly adaptive airfoil that enables demanding flight maneuvers, which are performed with an astonishing robustness under turbulent conditions, and stability at slow flight speeds. Recent wind tunnel experiments revealed that bat flight generates complex aerodynamic tracks with wake vortices, i.e., areas of turbulent, reverse airflow (5, 6). Hence, domed wing hairs, which resemble the haarscheibe rather than the classic Merkel-cell neurite complex (7), and the tactile receptors associated with them (Merkel receptors) might be specialized to sense airflow patterns and therefore help stabilize flight when airflow is disrupted (3, 4). Sensory sensilla on the wing and other body parts of insects have been shown to play a role in flight control (8, 9), as have vibrotactile receptors at the feather base of birds (10). Our goal was to study the role of the wing hairs of bats by combining anatomical, neurophysiological, and behavioral flight experiments that involved depilation of the hairs.

Results

Microchiropteran bats of the species *Eptesicus fuscus* (*E.f.*, big brown bat) and *Carollia perspicillata* (*C.p.*, short-tailed fruit bat) were used in these experiments. *E.f.* is an insectivorous species, commonly found throughout North America, and *C.p.*, a neotropical, frugi- and nectarivorous species, which is known to hover during foraging flight. First, the anatomy and distribution of the wing hairs were studied using a scanning electron microscope. We found that in *E.f.*, hairs can be found everywhere on the wing, but that there are two kinds of hairs. The first type of hair is long (up to several millimeters), relatively thick (6–18 μm), and found close to the ventral forearm, around the leg, and on the tail membrane (IFM), resembling pelage hair. On the other membranous parts of the wing, a second type of hair was found, which is invisible to the naked eye. Fig. 1 shows an example of these hairs collected from *E.f.* This type of hair is very short (100–600 μm), with the shortest ones found along the trailing edge of the wing. They are so thin that only one follicle cell builds each segment of the hair, resulting in a coronal scale pattern. The tip diameter of these hairs is only 200–900 nm. These small hairs are typically found in rows, generating a sparse grid of about one hair per mm^2. In *C.p.*, the distribution of the hairs, as well as their length and thickness, are similar except that in some areas of *C.p.*'s wing membrane, several hairs protrude from one dome.

Electrophysiology. To characterize the physiological properties of the wing hairs, we recorded multineuron cluster responses to airflow or direct tactile stimulation of the wing membrane in the primary somatosensory cortex (S1) of *E.f.* First, the tactile receptive fields were measured using handheld calibrated monofilaments (von Frey hairs). Then, a cannula was pointed at the center of the receptive field at a distance of 3 mm. An airflow generator produced calibrated, triggered air puffs of 40-ms duration. The magnitude of the air puffs was adjusted to be just above the response threshold of the neuronal cluster (20–30 mm/s), assuring that the air puff would not move or deflect the wing membrane in addition to the hairs, and thereby potentially activate other cutaneous tactile receptors, e.g., stretch receptors, than those associated with the hairs. For details of air puff calibration and diameter of stimulated wing surface see *Materials and Methods*. The neuronal response to air puffs from eight directions (20 trials each) was recorded, the hairs were removed using depilatory solution, and the neuronal response was recorded again (Fig. 2). Air puffs elicited a slowly adapting response in S1 neurons, which is consistent with earlier primary afferent recordings (3, 4). After depilation, S1 response to air puffs disappeared for all of the seven tested membrane sites in two bats, whereas the responses to direct tactile stimulation of the skin were still intact and showed the typical fast-adapting characteristic of wing stretch receptors, which have been previously described to be highly sensitive to any membrane deformation but relatively insensitive to airflow (3, 4). The responses of S1 neurons to the airflow were clearly directional, and the preferred direction varied with wing location (Fig. 3), with the entire trailing edge and the midwing area most sensitive to airflow from the rear, which suggests that this area might be most sensitive to wake vortices (turbulent, inverse airflow), when the laminar flow of air is disrupted (5, 6). We draw three conclusions from the electrophysiological experiments. Firstly, the depilatory solution

Author contributions: S.S.-D., J.M.Z., and C.F.M. designed research; S.S.-D., M.C., C.C., B.F., W.X., J.B., J.M.Z., and C.F.M. performed research; S.S.-D., M.C., C.C., B.F., W.X., and J.B. analyzed data; and S.S.-D. and C.F.M. wrote the paper.

The authors declare no conflict of interest.

*This Direct Submission article had a prearranged editor.

[1]To whom correspondence should be addressed. E-mail: ssterbin@umd.edu.

SYSTEMS BIOLOGY

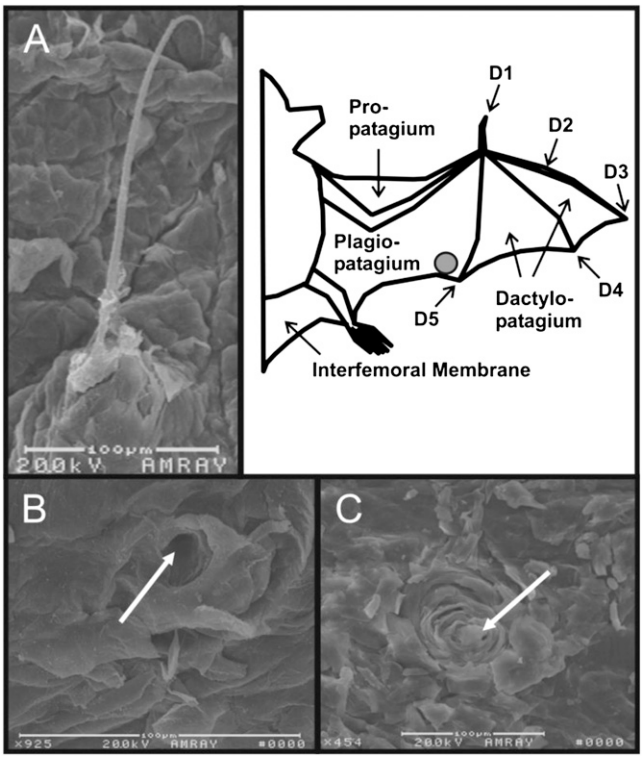

Fig. 1. Sensory wing hair before (*A*) and after (*B* and *C*) depilation. (*A*) Scanning electron microscope image from a domed hair located on the ventral trailing edge (location is marked by a gray circle in schematic to the *Right*) of *Eptesicus fuscus*. Note the calibration bar below the photomicrograph for reference. (*Right*) Schematic of the bat wing and its parts. (*B* and *C*) Examples of domes after depilation. Arrows point to the center of the domes from which the hair would normally protrude.

removes the hairs, but does not affect the function of other tactile receptors in the wing membrane. The complete removal of the hairs was microscopically confirmed in each case. Secondly, the deflection of the hairs caused by low-intensity air puffs activates the receptors (Merkel cells) at the base of the hairs, and the hairs are indeed involved in sensing airflow in a directional pattern. Thirdly, the pattern of preferred directions across the wing indicates that these hairs detect reverse, turbulent airflow, and therefore might be involved in stabilizing flight.

Flight Performance Testing. We addressed the question of whether removal of the hairs would affect flight performance. The two bat species, *E.f.* and *C. p.*, were used to study the role of wing hairs in flight control for obstacle avoidance. In a flight room, dimly lit with long-wavelength red light, *E.f.* was trained to fly through an artificial forest of columned vertical transparent nets, relying on echolocation, to be rewarded with a tethered mealworm that was positioned at random locations (Fig. 4). *C.p.* was trained to fly through openings in a series of nets to create a maze and was rewarded with banana (Fig. 5*A*, *Inset*). Flight behavior was monitored with two high-speed IR-sensitive video cameras mounted in corners of the room. With the stereo video recordings, we are able to reconstruct the 3D flight paths of the bats. First, baseline data were collected, then wing hairs were removed from different functional regions (trailing edge, leading edge, midwing) of the wing. Flight testing was completed on the same day as hair removal or the subsequent day to exclude compensatory plasticity in the flight behavior. Fig. 4 shows flight paths of one *E.f.* before and after removal of hairs along the entire trailing edge of the wing, from the very edge to 2 cm into the wing from wing tip to tail tip on both sides. The flight traces marked in blue show that this bat makes wider turns and does not maneuver as closely to the trees than before hair removal. Also, both specimens of *C.p.* increased maximum average flight speed, from about 2.5 m/s to about 3.5 m/s, most pronouncedly during the initial flight phase when the trailing edge is depilated (Fig. 5*A*). Additional depilation of the hairs on the leading edge and midwing did not lead to a further increase of speed, indicating that the trailing edge sensors are crucial for slow flight speed. Also in *C.p.* the average turn angle is reduced after depilation (Fig. 5*B*). Fig. 5 *C* and *D* illustrate the relationship between average flight speed, turn angle, and obstacle distance along the flight path (based on the same raw dataset). Apparently, the relationship between speed and turn angle is not linear, but depends on the phase of the flight path. Following launch, the bat speeds up and heads toward the obstacle, making only wide turns. After the travel speed is reached, the turn angle systematically decreases with increasing speed. After depilation of the different wing areas (three colored curves), the bats' peak turn angle is only between 2.4 and 3.6 ° compared with 5 ° during the baseline trials (Fig. 5*C*). Fig. 5*D* illustrates the relationship between average flight speed and average distance to the obstacle. After depilation (colored curves) flight speed is increased at all distances. The maximum average distance before treatment is 0.87 m; after treatment, it is 1.33–1.44 m.

Discussion

Our data indicate that the hairs in the bat wing membrane play a crucial role in the maneuverability tasks, especially during slow flight. The flight performance after depilation shows that wing hair removal along the trailing edge alone statistically causes the same effects as the depilation of the entire wing. This finding is in accordance with a study that showed that the domed hairs on bat wings are associated with membrane areas subject to higher turbulence and flow reversal associated with flow separation (11). Removing the tactile wing hairs of the trailing edge makes a bat increase speed and reduce turn angle (i.e., make wider turns). We interpret the depilated bats' increase in flight speed as the result of the lack of input from the domed hair receptors to the somatosensory system. A simple explanation for this increase might be that the hairs function as flight velocity sensors, and the depilated bat would interpret a lack of input from the hairs as low speed and consequently increase the flight speed.

However, our findings that neural responses to airflow are directional suggest that wing sensors may play a role in stall detection. In the behavioral task a depilated animal may attempt to avoid a stall by speeding up, because sensory inputs indicating reverse airflow have been disrupted. Although comparing bat flight to fixed-wing aircraft flight is problematic, and it is unknown whether juvenile bats "learn" to avoid stalls when they start flying, increasing air speed is also recommended to aircraft pilots to recover from stalls (12). We never observed a bat actually stall and crash after depilation. This could be explained by kinesthetics and proprioceptive inputs, which are still available after removal of the hairs. It also remains an open question whether a bat can adapt to the absence of wing hairs over time. We tested the flight performance within 2 d of depilation. It is unclear whether, and in which time frame, the domed hairs grow back. Visual control of the wing surface with light microscope and SEM confirmed that the hairs were removed. In the SEM, the embedded bases of the hairs were frequently visible; hence it is unlikely that the short application of depilatory cream affects the interior of the domes. Transmission electron microscopy revealed that the Merkel cells surrounding the hair follicle are deeply embedded in the skin (13). After depilation of the hairs, the tactile responses to stimulation with monofilaments are still robust, which means that tactile receptors are intact. Obviously, stimulation with monofilaments indents the skin and therefore

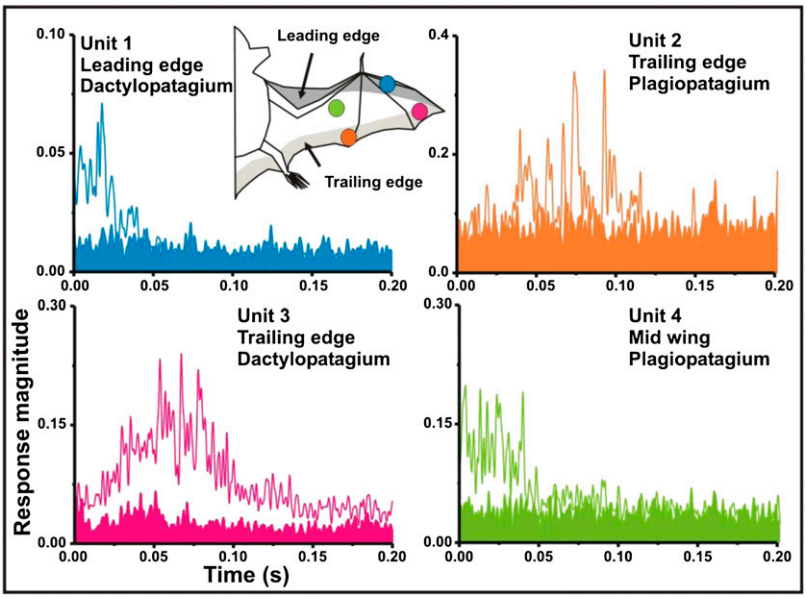

Fig. 2. Cortical responses to airflow stimulation are diminished after depilation. The averaged poststimulus multiunit responses (time 0, end of air puff) to 10 air puff stimulations are shown for four different wing locations (see color-matched circles in bat schematic; open line, before depilation; filled area, after depilation). During the recording after hair removal, it was first tested whether the center of the tactile receptive field was still in the same location on the dorsal wing surface as before the depilation.

affects a variety of tactile receptors, possibly also the Merkel cells at the hair follicle in the domes. However, the domed wing hairs are so sparsely distributed (1/mm^2) that other receptor types of the skin outnumber these hair-associated Merkel cells by far, and therefore contribute more input to the neuronal response. Of importance is the finding that the low-level airflow—which does not indent the skin—does not elicit a response after depilation, whereas the tactile response elicited by the monofilament—which does indent the skin—is still robust. This suggests that airflow causes a deflection of the hairs that in turn stimulate the Merkel cells, even at very low airflow speeds. Of course they also respond to stronger airflow, but in this case we would not be able to distinguish between stimulation via the leverage of the hairs or simple indentation of the skin, which presumably would be omnidirectional.

Our findings also trigger some interesting evolutionary questions. In mammals, tactile hairs are usually located on the head in the form of sinus hairs (e.g., whiskers). Sinus hairs on other body parts have been described only for the manatee (14). The authors suggested that the sparsely distributed hairs on the manatee's body could form a lateral line system analogous to that of fish and amphibians, where it serves to detect water currents surrounding the animal's body. However, the hairs we found on the bat wing are clearly not sinus hairs (3, 4). Their small size suggests that they may be specialized vellus hairs (15). Merkel cells detect the direction, amplitude, and duration of deflection of the hair (16). Interestingly, the tactile wing hairs of the bat are found on both surfaces of the dactylopatagium, the membrane between the fingers, indicating that the bat's ventral hand surface is not glabrous, e.g., hairless, in contrast to other nonhoofed mammals such as primates or rodents. Furthermore, the plagiopatagium, which grows from the bat embryo's flank (17) and forms a large portion of the bat's wing membrane, is covered by the same type of hair as the dactylopatagium. This finding suggests that the entire wing membrane, although in part derived from embryonic body parts other than the upper extremity, is surprisingly homogeneous with respect to these specialized tactile hairs.

Hairs, feathers, or other hair-like structures are commonly found on the wings of animals capable of powered flight. In insects a dense grid of very short hair-like structures on the wing are thought to primarily make the wing water repellent (18). Flight control is achieved by different structures, some of which are located at the wing base or on the wing margin, others are located elsewhere on the insect's body. Campaniform sensilla, which are domed structures without a protruding hair, on the wing of the blowfly detect deformation of the entire wing blade, but not airflow (19). Recently described bristles along the wing margins of the silkworm moth, typical mechanosensilla with a single receptor neuron, respond to vibration but not constant air currents as used in the present study (20). In contrast, airflow sensitive hairs are found on the head (8) or prosternum of many insects (9). The sensory afferent neurons that innervate these airflow sensitive hairs make monosynaptic connections with an identified interneuron that contacts motor neurons for controlling wing angle during flight (21). Flight stabilization of many insects typically involves vibrating structure gyroscopes like for example halteres, the modified rear wings of two-winged insects, Diptera (22–24). Recent studies revealed that mechanoreceptors located on the antennae might provide a similar function for four-winged insects (25).

Flying vertebrates lack such specialized gyroscope organs, but tactile sensors distributed over the wing surface might nevertheless serve the same purpose of flight control. Microscopic analysis of the Pterosaur wing membrane showed that the patagium was covered with ultrafine hair-like structures, with a diameter of only 0.01 mm, whose function remains subject to speculation (26). Birds have vibrotactile Herbst corpuscles at the feather bases that aid in flight control (10, 27), but no Merkel receptors, which are found only in featherless skin (28). Therefore, we conclude that the Merkel cell-associated hairs on the bat wing might represent a unique evolutionary feature for flight control.

Materials and Methods

Animals. *E. fuscus* were wild-caught in Maryland. *C. perspicillata* were donated (Montréal Biodôme, Montreal, QC, Canada). Bats were housed under reversed 12 h light/dark conditions. *C.p.* were maintained on a diet of various

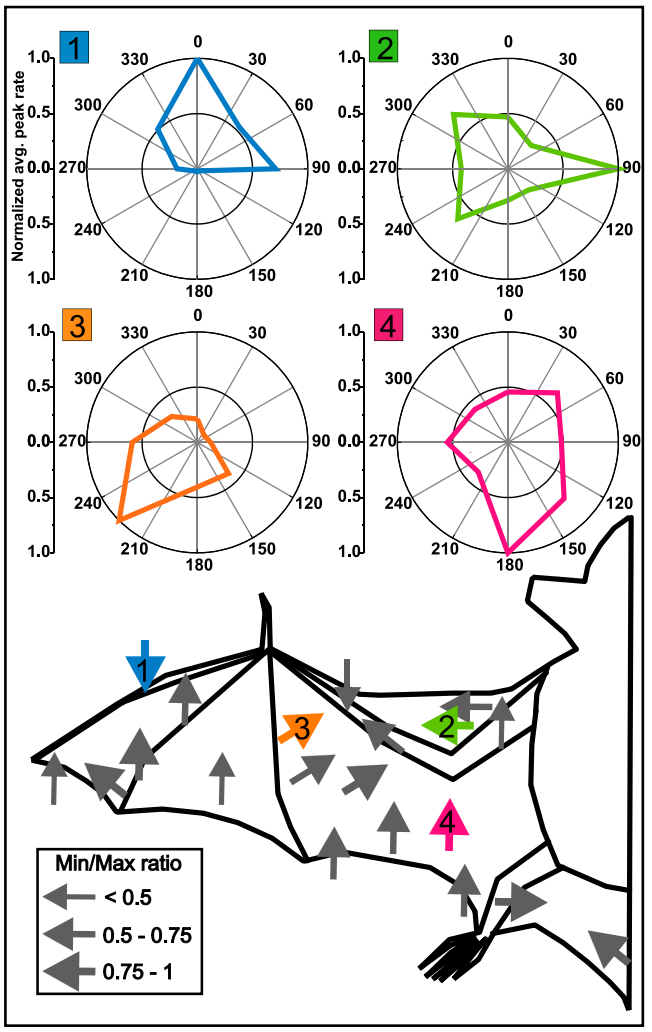

Fig. 3. Directionality of responses to airflow in primary somatosensory cortex of *Eptesicus fuscus*. *Top* shows the directional responses of four multineuron clusters as polar plots. Airflow from each of the eight directions (every 45 °) was presented 20 times. The polar plots show the averages of the neuronal peak response, normalized to the peak. (*Lower*) Locations of the center of the receptive field (tip of arrow) for all tested neurons ($n = 20$). The arrows point in the direction of airflow that excites the neurons most at each location. The four colored arrows indicate the wing locations for the neuronal responses (*Upper*). Arrow thickness indicates the minimum–maximum ratio of the directional response strength. For example, a value of 0.5 indicates that for the nonpreferred direction the neuronal response was reduced by half compared with the preferred direction. Note that most neuronal clusters are tuned strongly with ratios between 0.5 and 1.

fruits and water. Banana was provided only during experiments. *E.f.* were maintained on a diet of mealworms, *Tenebrio molitor*, and water. Mealworms were only provided during experiments. All procedures were approved by the University of Maryland Institutional Animal Care and Use Committee.

Scanning Electron Microscopy. Circular samples (13-mm diameter) from 24 different parts of the wing of two *E.f.* (12 each), 8 samples from the wing of one *C.p.* at corresponding locations except tail membrane were taken and fixated in 2.5% glutaraldehyde solution, washed in phosphate buffer (PBS), and then fixated in 1% osmium tetroxide in PBS (60 min). After standard washing procedure with bidistilled water and dehydration in 75, 95, and 100% ethanol, the samples were dried in a critical point dryer (Denton; DCP-1). The samples were mounted onto metal pedestals with silver paste, placed in a 50 °C oven to harden, and then coated with gold palladium alloy (Denton; DV-502/502 vacuum evaporator). The samples were viewed in a scanning electron microscope (Amray; AMR-1610).

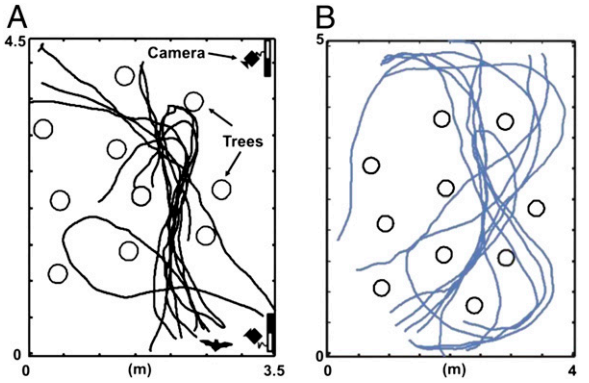

Fig. 4. Flight experiments before and after wing hair removal in *Eptesicus fuscus*. The bat was trained to fly through a group of artificial trees to catch a tethered mealworm. Videos from two infrared-sensitive high-speed cameras were used to reconstruct the flight paths. (*Left*) Ten flight paths recorded over 10 trials before hair removal (viewed from top). (*Right*) Ten flight paths after removal of all tactile hairs along dorsal and ventral trailing edge (2-cm width of depilated wing membrane on each side). Note that the bat makes wider turns, i.e., the turn angle per frame decreased.

Neurophysiology. Electrophysiological recordings were made in six *E.f.* The bats were initially anesthetized with 3% isoflurane (700 cc/min O_2) and anesthesia was maintained at 1–3% level during surgery and cortical recordings. Breathing rate and body temperature (maintained around 37 °C) were monitored. A midline incision exposing the skull was made and muscles deflected from the midline. A stainless steel headpost was glued to the skull above the olfactory bulb using cyanoacrylate (Loctite 4161). Bats were allowed to recover for 2–3 d before physiological recordings.

The headpost was used to secure the head to a vibration isolation table (Kinetic Systems). A craniotomy was performed over the primary somatosensory cortex (S1) according to stereotaxic coordinates. Application of sterile saline prevented desiccation of the exposed brain surface. A low-impedance (~1 MΩ) tungsten reference electrode was inserted into a nonsomatosensory region of the opposite hemisphere. A high-impedance tungsten electrode (15–20 MΩ; FHC) was used to record extracellularly from multiunit (MU) clusters. The electrode was attached to three digital micromanipulators (Mitutoyo) for exact measurement of recording depth rostrocaudal and mediolateral position. The contralateral wing was spread and taped by the tip to the stereotaxic frame.

Multiunit recordings were made from several perpendicular electrode penetrations across the area of S1 that responds to tactile stimulation of different parts of the dorsal wing membrane. We decribed the details of wing representation in the primary somatosensory cortex of *E. fuscus* in an earlier publication (29). For each recording position, stimulation was performed with handheld monofilaments (North Coast) that apply calibrated pressure (0.008–1 g). The tactile receptive field (RF), i.e., the area of the wing that elicits a response, was measured. The center of each RF was defined as the membrane location that responded to the lowest filament weight (neuronal threshold). For stimulation with air puffs, a blunt syringe (14 gauge, inner diameter 1.6 mm) was directed at the RF center from different angles in 45 ° steps. Air puff stimuli were generated by an electronic high precision dispensing workstation (Nordson EFD; Ultra 2400 Ultimus) that allows exact adjustment of dispense time (stimulus duration) and pressure of gases and fluids. Time increment adjustments can be as small as 0.0001 s for precise deposit control. The air output ranges from 0 to 100 psi (0–6.9 bar). The air puff duration was 40 ms in all experiments. Airflow velocity was calibrated with an anemometer (Datametrics; 100VT-A) at a 3-mm distance to the syringe opening, the same distance (syringe opening to wing membrane) that was used during the experiments. The area of the wing affected by the air puff was estimated using the displacement of talc powder on a paper surface as reference. At air puff magnitudes close to the neuronal threshold (20–30 mm/s, 2 psi), the diameter of the affected area is about 8 mm in the direction of the syringe, as well as orthogonally. With a known density of one hair per mm^2 (our SEM analysis), we conclude that a maximum of 64 hairs were deflected. In comparison to the average size of the tactile receptive fields of the wing membrane, this area is small. For the recording after depilation, the effective diameter of the air puffs is irrelevant, because the entire wing surface was depilated. Also, because of the great distance

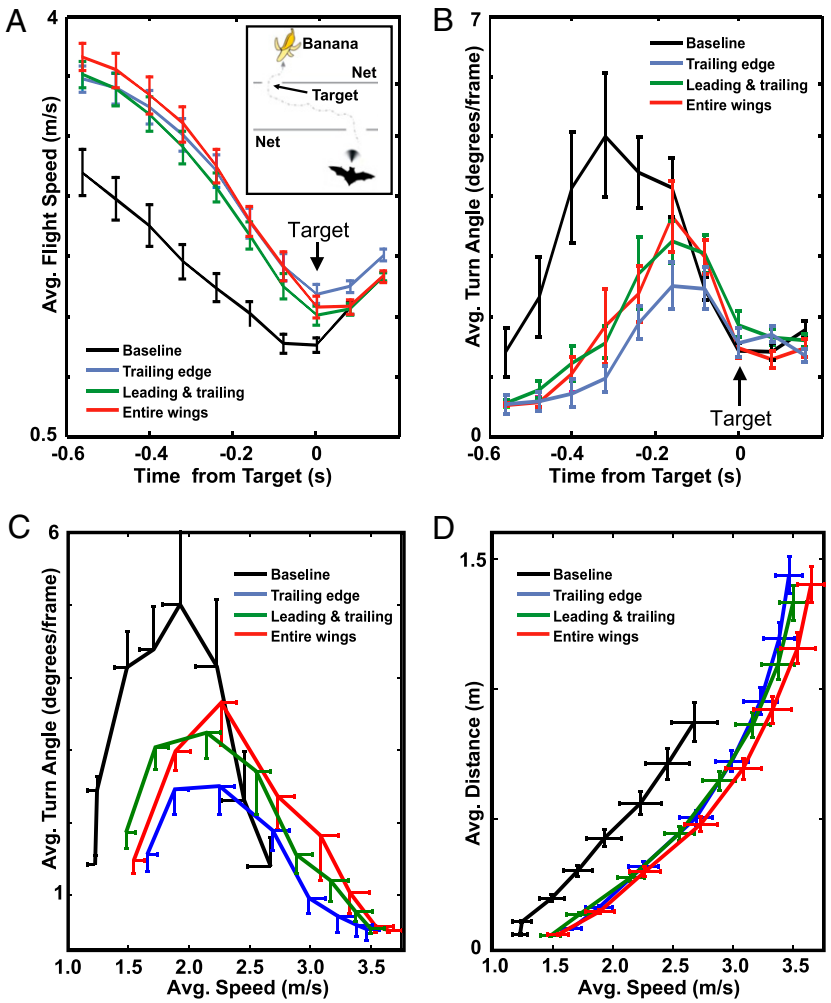

Fig. 5. Flight experiments before and after wing hair removal in *Carollia perspicillata*. The bats had to fly through openings in two parallel nets to get a food reward (banana, *Inset*). (*A*) Flight speed was increased after hair removal along the trailing edge (black vs. blue line), (two animals, 117 trials, mean ± SE). Additional depilation of the leading edge (red) and midwing areas (green) did not further increase flight speed. (*B*) Conversely, the average turn angle of the bats decreased with wing hair depilation, indicating that their maneuverability was negatively affected (same trials as for *A*). (*C*) Flight speed vs. turn angle. After treatment the average maximum speed (mean ± SE) is increased and the maximum turn angle reduced. The bats generally make wider turns. (*D*) Flight speed vs. obstacle distance. The maximum distance to the obstacles is 16–25% greater after treatment.

between individual hairs with on average one hair per mm^2 with a hair diameter at the base of 5–6 μm and the known length range, nonlinear coupling between the hairs can be excluded if the distance is greater than 50 hair diameters (30, 31), which would be in our case around 275 μm.

At each recording site, the magnitude of the air puff was adjusted to be just above the neuronal threshold, usually set to 20–30 mm/s airflow speed, ensuring by microscopic inspection that no indentation of the membrane occurred. The workstation trigger also started the data acquisition board that recorded the waveform of the neural responses after amplification (Bak Electronics) and band-pass filtering (400–4,000 Hz; Stanford Research Systems). Each stimulus was presented 10 times (depilation experiment, Fig. 2), or 20 times (airflow directionality experiment, Fig. 3). The MU responses (entire waveforms) were half-wave rectified and averaged. The responses for each stimulation direction were normalized to maximum and plotted as polar diagrams. Minimum–maximum ratio between the best (preferred) and worst direction was calculated to quantify the strength of directionality of the air puff response of 20 MUs from four *E. fuscus*.

In two bats, all hairs on the dorsal wing surface were depilated after collecting the baseline data (depilation method see below). Two days later, the electrode was inserted in the same (±50 μm) cortical region again using the three stereotaxic coordinates relative to a benchmark. Monofilament and air puff stimulation were repeated as described above. At the end of the recording sessions (4–6 h), the bats were killed with sodium pentobarbital.

Flight Experiments. Flight path recordings were conducted in a carpeted flight room (7 × 6 × 2.5 m) with acoustic foam on walls and ceiling (Sonex). Low-intensity, long-wavelength light (>650 nm, incandescent bulbs filtered through Plexiglas G 2711; Atofina Chemicals) allowed the use of two high-speed (250 fps) infrared video cameras (FASTCAM-PCI-R2) for 3D position determination of bat and obstacles.

The task for *E.f.* was as follows: An artificial forest was created in the flight room using 10 simulated tree trunks (1.2 and 1.7 trees/m^2). Each tree consisted of two metal rings (diameter 25.4 cm), which formed the top and bottom. The rings were connected with string (length 2.1 m) and wrapped with mist net (Avinet 38 mm mesh 75 denier/2-ply). The bat was trained to fly through the forest and capture tethered mealworms. Ten trials were collected before treatment on one day and eight trials were collected after treatment on a different day. The video system was end triggered at the completion of a trial. For the experimental condition, hairs were removed using depilatory cream (Veet 3-min formula) on the ventral and dorsal surface of the trailing edge of the wing and the ventral tail membrane.

The task for *C.p.* (two animals) was as follows: Two mist nets (same as above) were hung from the ceiling to section the room into three compartments. Each net had an opening (~22 × 30 cm) for the bats to fly through to access a food reward (banana hanging from the ceiling by a metal skewer) behind the second opening. The openings were located on opposite ends of the nets forcing the bat to make sharp turns. A trial consisted of the bat flying directly

from one end of the room to the other, passing through both net openings, and landing on the banana. Baseline data were collected first (27 trials). For the experimental conditions wing hairs were depilated (Veet 3-min formula, 50% diluted, applied for 2 min, rinsed off, with water) from subsequent wing areas over a period of a few weeks. The wing was allowed to dry completely before experimental trials commenced. First, hairs from the entire dorsal surface of the wing and the trailing edge of the ventral surface (29 trials) were removed. Second, hairs from the leading edge of the ventral wing surface (34 trials) were removed. Third, hairs from the midventral wing surface (27 trials) were removed, resulting in a completely depilated wing membrane.

ACKNOWLEDGMENTS. We thank Tim Maugel for assistance with SEM and Scott Livingston for help with behavioral studies. This research was supported by Air Force Office of Scientific Research Multidisciplinary Research Program of the University Research Initiative (MURI) Grant "Biologically Inspired Flight for Micro-Air Vehicles."

1. Maxim H (1912) The sixth sense of the bat. Sir Hiram's contention. The possible prevention of sea collisions. *Sci Am* 27:80–81.
2. Griffin DR, Galambos R (1941) The sensory basis of obstacle avoidance by flying bats. *J Exp Zool* 86:481–506.
3. Zook JM (2005) The neuroethology of touch in bats: Cutaneous receptors of the wing. *Soc Neurosci Abstr* 78.21.
4. Zook JM, Fowler BC (1986) A specialized mechanosensory array of the bat wing. *Myotis* 23-24:31–36.
5. Hedenström A, et al. (2007) Bat flight generates complex aerodynamic tracks. *Science* 316:894–897.
6. Muijres FT, et al. (2008) Leading-edge vortex improves lift in slow-flying bats. *Science* 319:1250–1253.
7. Smith KR, Jr. (1977) The Haarscheibe. *J Invest Dermatol* 69:68–74.
8. Haskell PT (1958) Physiology of some wind-sensitive receptors of the desert locust (*Schistocerca gregaria*). *XVth Int Zool Congr* (London), pp 960–961.
9. Pflueger HJ, Tautz J (1982) Air movement sensitive hairs and interneurons in *Locusta migratoria*. *J Comp Physiol A Neuroethol Sens Neural Behav Physiol* 145:369–380.
10. Necker R (1985) Receptors in the wing of the pigeon and their possible role in bird flight. *Biona Rep 3: Vogelflug*, ed Nachtigall W (Fischer, Stuttgart), pp 433–444.
11. Crowley GV, Hall LS (1994) Histological observations on the wing of the grey-headed flying fox (Pteropus poliocephalus) (Chiroptera: Pteropodidae). *Aust J Zool* 42: 215–231.
12. Federal Aviation Administration (FAA) (2007) *Airplane Flying Handbook* (Skyhorse Publishing, New York), 2nd Ed.
13. Zook JM (2006) *Evolution of Nervous Systems. Vol. 3: Somatosensory Adaptations of Flying Mammals*, ed Kaas JH (Academic, Oxford), pp 215–226.
14. Reep RL, Marshall CD, Stoll ML (2002) Tactile hairs on the postcranial body in Florida manatees: A Mammalian lateral line? *Brain Behav Evol* 59:141–154.
15. Halata Z (1993) Sensory innervation of the hairy skin (light- and electronmicroscopic study. *J Invest Dermatol* 101 (1, Suppl):75S–81S.
16. Gottschaldt KM, Iggo A, Young DW (1973) Functional characteristics of mechanoreceptors in sinus hair follicles of the cat. *J Physiol* 235:287–315.
17. Cretekos CJ, et al. (2005) Embryonic staging system for the short-tailed fruit bat, Carollia perspicillata, a model organism for the mammalian order Chiroptera, based upon timed pregnancies in captive-bred animals. *Dev Dyn* 233:721–738.
18. Wagner P, Neinhuis C, Barthlott W (1996) Wettability and contaminability of insect wings as a function of their surface sculptures. *Acta Zool* 77:213–225.
19. Dickinson MH (1990) Comparison of encoding properties of campaniform sensilla on the fly wing. *J Exp Biol* 151:245–261.
20. Ai H, Yoshida A, Yokohari F (2010) Vibration receptive sensilla on the wing margins of the silkworm moth Bombyx mori. *J Insect Physiol* 56:236–246.
21. Watson AHD, Pflüger HJ (1994) Distribution of input synapses from processes exhibiting GABA- or glutamate-like immunoreactivity onto terminals of prosternal filiform afferents in the locust. *J Comp Neurol* 343:617–629.
22. Loew H (1858) Ueber die Schwinger der Dipteren. *Berl Ent Zeitschr* 2:225–230.
23. Fraenkel G (1939) The function of the halteres of flies. *Proc Zool Soc Lond A* 109: 69–78.
24. Dickinson MH (2005) The initiation and control of rapid flight maneuvers in fruit flies. *Integr Comp Biol* 45:274–281.
25. Sane SP, Dieudonné A, Willis MA, Daniel TL (2007) Antennal mechanosensors mediate flight control in moths. *Science* 315:863–866.
26. Padian K, Rayner JMV (1993) The wings of pterosaurs. *Am J Sci* 293:91–166.
27. Hoerster W (1990) Histological and electrophysiological investigations on the vibration-sensitive receptors (Herbst corpuscles) in the wing of the pigeon (*Columba livia*). *J Comp Physiol A Neuroethol Sens Neural Behav Physiol* 166:663–673.
28. Saxod R (1978) Development of cutaneous sensory receptors in birds. *Handbook of Sensory Physiology. Development of Sensory Systems*, ed Jacobson M (Springer, Berlin), pp 337–417.
29. Chadha M, Moss CF, Sterbing-D'Angelo SJ (2011) Organization of the primary somatosensory cortex and wing representation in the Big Brown Bat, *Eptesicus fuscus*. *J Comp Physiol A Neuroethol Sens Neural Behav Physiol* 197:89–96.
30. Cummins B, Gedeon T, Klapper I, Cortez R (2007) Interaction between arthropod filiform hairs in a fluid environment. *J Theor Biol* 247:266–280.
31. Heys JJ, Gedeon T, Knott BC, Kim Y (2008) Modeling arthropod filiform hair motion using the penalty immersed boundary method. *J Biomech* 41:977–984.